SCIENTIFIC REPORTS

OPEN

SUBJECT AREAS:
ELECTROCATALYSIS
MATERIALS SCIENCE

Received
27 October 2014

Accepted
16 December 2014

Published
15 January 2015

Correspondence and requests for materials should be addressed to X.F. (xjfeng2011@sinano.ac.cn)

Rhodium Nanoparticle-mesoporous Silicon Nanowire Nanohybrids for Hydrogen Peroxide Detection with High Selectivity

Zhiqian Song, Hucheng Chang, Weiqin Zhu, Chenlong Xu & Xinjian Feng

Nanobionics Division & Key Laboratory of Nano-Bio Interface, Suzhou Institute of Nano-Tech and Nano-Bionics, Chinese Academy of Sciences, Suzhou 215123 China.

Developing nanostructured electrocatalysts, with low overpotential, high selectivity and activity has fundamental and technical importance in many fields. We report here rhodium nanoparticle and mesoporous silicon nanowire (RhNP@mSiNW) hybrids for hydrogen peroxide (H_2O_2) detection with high electrocatalytic activity and selectivity. By employing electrodes that loaded with RhNP@mSiNW nanohybrids, interference caused from both many electroactive substances and dissolved oxygen were eliminated by electrochemical assaying at an optimal potential of +75 mV. Furthermore, the electrodes exhibited a high detection sensitivity of 0.53 μA/mM and fast response (< 5 s). This high-performance nanohybrid electrocatalyst has great potential for future practical application in various oxidase-base biosensors.

Developing electrocatalysts with high activity and selectivity for H_2O_2 detection is of both academic and industrial importance because H_2O_2 is the product of most oxidase catalyzed bioreactions and is commonly used for the determination of various clinical important substrates[1]. Electrochemical assay is a simple, rapid and effective approach[2]. Electrochemical detection of H_2O_2 can be achieved via either anodic oxidation or cathodic reduction. Despite many advantages, anodic H_2O_2 measurement suffers from interference caused from endogenous species, such as ascorbic, urea and uric acids that can be electro-oxidized at a similar potential[3,4]. Consequently, the detection selectivity and accuracy are affected. In order to minimize such interference, one common route is to use electrocatalysts that allow electro-oxidation of H_2O_2 at lower potential. Transition metals[5–8], metal porphyrins[9,10], redox polymers[11,12], graphene[13,14] and carbon nanotubes[15–17] have thus been employed. Although significant advances have been made, detection error still exists because some easily oxidized substances, such as ascorbic acid (AA) is electroactive even at potential of as low as +150 mV[18]. These interferences accompanying H_2O_2 electro-oxidation can be eliminated if H_2O_2 is measured via electrochemical reduction[19,20]. But cathodic detection of H_2O_2 is normally interfered by dissolved oxygen that can be reduced at a similar potential[21–23]. Therefore, it is highly desirable but yet a challenge to fabricate electrode materials that can inhibit the interferences caused from both endogenous species and dissolved oxygen. Here, we report rhodium nanoparticle-mesoporous silicon nanowire (RhNP@mpSiNW) nanohybrids for H_2O_2 detection with high selectivity and sensitivity via cathodic reduction. At an operating potential of +75 mV, interferences caused from the oxidation of endogenous substrates and the reduction of dissolved oxygen were both eliminated.

Results

RhNP@mpSiNW nanohybrids were prepared via a two-step approach. Firstly, mpSiNWs were prepared via a metal-assisted chemical etching approach[24,25]. Figure 1a is a typical field emission scanning electron microscopy (FE-SEM) cross-sectional view of the as-synthesized mpSiNW arrays. The NWs have homogenously distributed nano-pores with an average size of about 15 nm as revealed from the transmission electron microscopy (TEM) shown in Supplementary Fig. S1a. The continuous crystal lattices across these nano-pores shown in Supplementary Fig. S1b indicate a single crystal feature of the as-prepared mpSiNWs. After the as-prepared NWs were scratched off from the silicon substrate they were loaded with RhNPs via chemical reduction approach using $NaBH_4$ as a reducing agent. As revealed from Figure 1b, a typical SEM image of RhNP@mpSiNW nanohybrids, small size of RhNPs are distributed on the side surface of mpSiNW. TEM image shown in

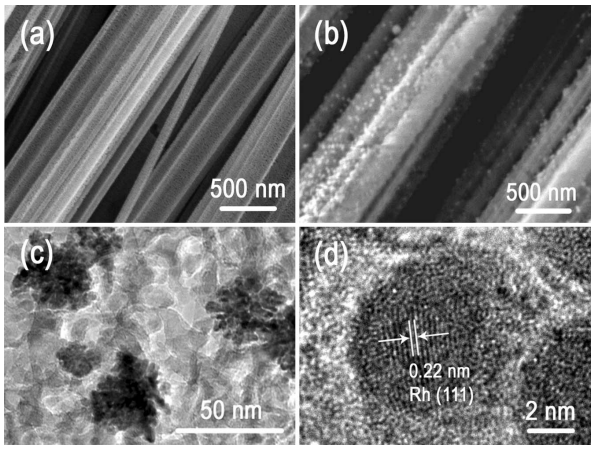

Figure 1 | FE-SEM images of the mpSiNWs (a) before and (b) after RhNPs loading. (c) TEM image of the RhNP@mpSiNW nanohybrid. (d) HR-TEM image of the RhNP@mpSiNW nanohybrid, indicating that each of the Rh NPs is highly crystallized.

Figure 1c indicates that the large RhNP is aggregation of small particles with size of 4–6 nm. Each of these small particles is single crystal as can be seen from the high resolution TEM (HR-TEM) image shown in Figure 1d.

The as-prepared nanohybrids were loaded onto glassy carbon (GC) electrode for H_2O_2 measurement. Figure 2a shows the linear sweep voltammetry (LSV) scan of the RhNP@mpSiNW/GC electrode in an oxygen-free buffer (solid line), air saturated buffer (dash line) and oxygen-free buffer containing 1 mM H_2O_2 (dash dot line). In comparison to electrode response in oxygen-free buffer, only a slightly higher cathodic current was observed in air saturated buffer which can be attributed to reduction of dissolved oxygen. The cathodic reduction starts at the potential of around + 60 mV. In marked contrast, the electrode gives a significantly higher cathodic reduction current in oxygen free buffer containing 1 mM H_2O_2. This could be attributed to the high electrocatalytic activity of the RhNPs towards H_2O_2 reduction. From these results, it can be seen that the dissolved oxygen will have little effect on the cathodic reduction of H_2O_2 if electrode potential of more positive than + 60 mV is used. Figure 2b depicts two almost identical calibrated lines of the RhNP@mpSiNW/GC electrodes at + 75 mV for the reduction of H_2O_2 with different concentrations in the presence and absence of dissolved oxygen (their original electrode LSV responses in oxygen-free solutions to various concentrations of H_2O_2 are shown in Supplementary Fig. S2). The sensitivity can be calculated to be 0.53 μA/mM from the linear part of the calibration curve. Inset in Figure 2b is electrode responses in low concentration ranges. These results show that almost no influence caused from oxygen was observed over a broad range of H_2O_2 concentrations, which can be attributed to the high electro activity of nanohybrids to H_2O_2 reduction and the considerably suppressed cathodic reduction activity to oxygen.

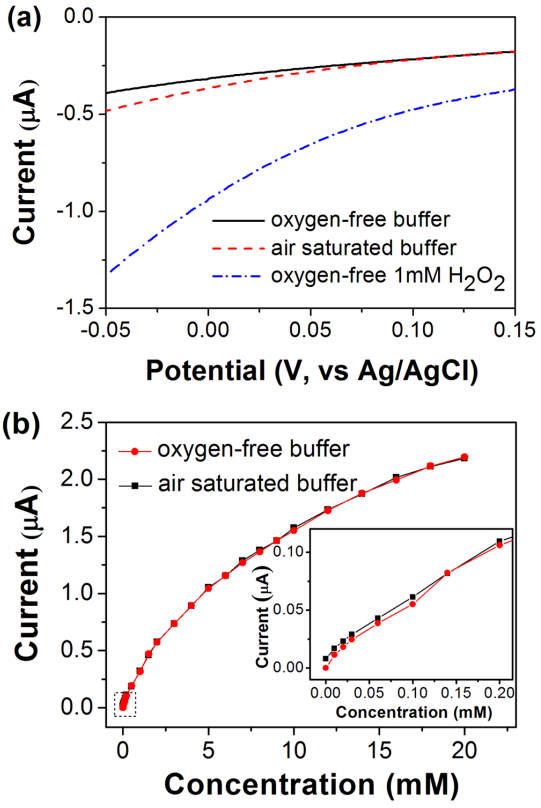

Figure 2 | (a) LSV response of the RhNP@mpSiNW/GC electrode with RhNP loading of 7.4 μg/mm² (loading percentage of Rh on mpSiNW is 22.7 wt%) in oxygen-free buffer, air-saturated buffer and oxygen-free buffer containing 1 mM H_2O_2 solution. (b) Plots of the current against H_2O_2 concentration in oxygen-free buffer and air-saturated buffer. Inset in (b) shows the magnified part marked with dash square. The experiments were performed at +75 mV.

Figure 3 shows a dynamic amperometric current-time response of RhNP@mpSiNW/GC electrode at +75 mV with a successive addition of H_2O_2 from 1 μM to 0.5 mM. The currents increase immediately and reached their equilibrium states rapidly after the addition of H_2O_2. The average rising time is less than 5 s, indicating a fast amperometric response towards H_2O_2 cathodic reduction. From the inset in Figure 3 we can see that the detection limit can be down to micro-mole range even in the presence of soluble oxygen. These results further reveal that the as-prepared RhNP@mpSiNW nanohybrids have good electrocatalytic activity towards H_2O_2 reduction and high selectivity against dissolved oxygen.

Figure 4a shows the current response of electroactive compounds of AA, urea and uric acid on RhNP@mpSiNW/GC electrode with different amount of RhNPs loading at potential of +75 mV during the measurement of 1 mM H_2O_2. The electrode amperometric response to H_2O_2 is not influenced by the addition of urea and uric acid in all three cases. The relative current responses of AA to that of H_2O_2 were as low as 4.5%, 2.2% and 1.0% with RhNP loading of 3.7, 7.4 and 11.1 μg/mm², respectively. Such behavior indicates that the activity towards H_2O_2 reduction increases with the increase of RhNP loading, while the response of AA is not sensitive to the RhNP loading variation. As a result, the relative current response of AA to that of

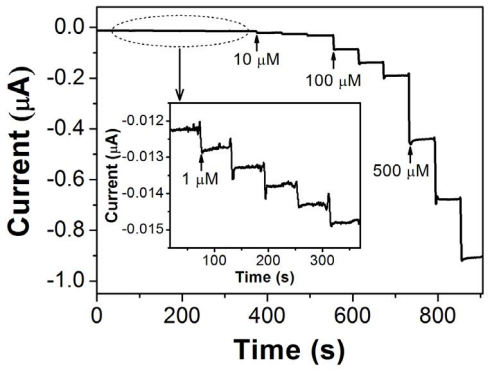

Figure 3 | **Amperometric responses of RhNP@mpSiNW/GC electrode in buffered solution after successive addition of H_2O_2 with different concentrations.** Inset: the magnified part of the curve marked with dash ellipse. The experiments were performed at +75 mV.

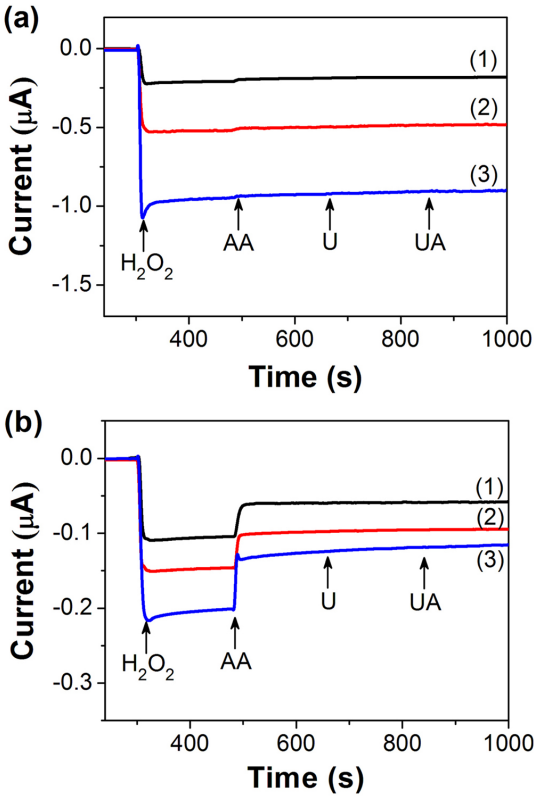

Figure 4 | Amperometric response of (a) RhNP@mpSiNW/GC and (b) RhNP loaded GC electrode with RhNP loading of (1) 3.7, (2) 7.4 and (3) 11.1 μg/mm² to 1 mM H_2O_2, 0.1 mM ascorbic acid (AA), 0.1 mM urea (U) and 0.1 mM uric acid (UA), respectively. The experiments were performed at +75 mV.

H_2O_2 decreases with the increase of RhNP loading. This indicates that the interference caused from AA, which is particularly challenging in oxidase-based biosensors, can be eliminated by using RhNP@mpSiNW nanohybrids based electrode with suitable amount of RhNP loading.

It is worth to note out that electrodes based on single-component RhNPs have been widely studied because of the relatively low operating anodic potential required for H_2O_2 detection, where current contributions of endogenous substances might be minimized. Figure 4b shows the current response of electroactive compounds of AA, urea and uric acid on RhNP loaded GC electrodes without mSiNWs at a potential of +75 mV. Significantly high anodic currents that resulted from the addition of AA were observed. The electrode output increases with the increase of RhNP loading upon the addition of both H_2O_2 and AA. The ratio of current response of AA to that of H_2O_2 can be calculated to be, respectively, as high as 39.6%, 29.6% and 32.0% for GC electrodes with RhNP loading of 3.7, 7.4 and 11.1 μg/mm², indicating that AA can be easily electro-oxidized at single-component RhNPs based electrode and bring current interference even at such a low potential. In marked contrast, as shown in Figure 4a, the interference caused from AA was significantly suppressed on nanohybrids modified electrode.

The stability of the RhNP@mpSiNW/GC electrode was further evaluated by continuous chronoamperometric measurements of 1 mM H_2O_2 at +75 mV. As shown in Supplementary Fig. S3, the electrode sensitivity is almost the same even after 50 time continuous measurements, indicating a good operational stability.

Discussion

In recent years, a large range of electrocatalysts have been developed in order to lower the H_2O_2 electro-oxidation potential so that interferences caused from electroactive species could be eliminated. Despite these efforts, detection error still exists because substances, such as AA are electroactive even at low anodic oxidation potential. Cathodic reduction is a promising approach that can avoid such interference during H_2O_2 detection. But, cathodic reduction lacks of reliability because the oxygen, whose concentrations are fluctuant in solution, can be reduced at similar potential. Mesoporous silicon nanowires are attractive for developing high-performance biosensors owing to their excellent semiconducting[26], mechanical[24], optical properties[27–29] and favorable biocompatibility[30,31]. In this work, the RhNP-mpSiNWs composite structure resulted in excellent selectivity against both many electroactive substrates and dissolved oxygen at an optimal potential of +75 mV. The remarkable selectivity against electroactive species of RhNP@mpSiNW can be attributed to the unfavorable electrostatic interaction between the mesoporous silicon and the probe molecular[32]. In a buffered solution with pH value of 7.2, the SiNW matrix covered with a large density of hydroxyl may bear a negatively charged surface and work as a permselective barrier that likely to prevent the negatively charged AA from reaching the electrode surface easily.

Conclusion

In this paper, RhNP@mpSiNW nanohybrids were prepared and their electro-catalytic properties were demonstrated. The amperometric detection of H_2O_2 was achieved by cathodic reduction at low potential of +75 mV, where acceptable low interferences caused from both dissolved oxygen and regular electroactive substances were achieved. Therefore, such nontoxic RhNP@mpSiNW nanohybrids are promising and have great potential for future practical artificial mediator free biosensor applications.

Methods

Chemicals. Hydrofluoric acid (HF, ≥40%), silver nitrate ($AgNO_3$, ≥99.8%), H_2O_2 (≥30%), sulfuric acid (H_2SO_4, 98%), nitric acid (HNO_3, 65% to 68%), sodium hydroxide (NaOH, ≥96%), sodium borohydride ($NaBH_4$, ≥99%), acetone, ethanol, potassium chloride (KCl, ≥99.8%), urea, uric acid and AA were purchased from Sinopharm Chemical Reagent Co., Ltd. Silicon (100) wafers (p-type, boron-doped, <1 Ω·cm) were purchased from Kaihua Lijing Silicon Materials Co., Ltd. The resistivity of the silicon wafers is 18.5 mΩ·cm according to square resistance measurement. Nafion and rhodium chloride ($RhCl_3$, 98%) were purchased from Sigma and used as received. All solutions were prepared with Milli-Q water.

Instrumentation and characterization. All electrochemical experiments were carried out with a CHI 660E (CHI Instruments Inc., Austin, USA). A conventional three-electrode system was used in this work. GC electrode, platinum wire and Ag/AgCl (3 M KCl) electrode were used as working, counter and reference electrode, respectively. Phosphate buffer with a concentration of 0.2 M (pH 7.2) was employed as the supporting electrolyte. Electrolyte solutions were bubbled with argon for at least 40 min and argon atmosphere was maintained over the solution during the deoxygenated electrochemical measurements. The microstructures of the samples were characterized using FE-SEM (S4800, Hitachi, Tokyo, Japan) and TEM Tecnai F20 (FEI, Hillsboro, OR, USA) electronic microscope at an accelerating voltage of 200 kV.

Preparation of mpSiNWs. Silicon (100) wafers (1.2 cm × 1.2 cm) were washed in a mixed solution of ethanol, acetone and water for 15 min and then immersed in a mixed solution of H_2SO_4 and H_2O_2 (v/v 3 : 1) for 10 min to remove surface organic materials. The wafers were then immersed in 8% HF solution for 10 min to form H-terminated surface and then dipped into a solution containing 8% HF and 8.3 mM $AgNO_3$ to coat a uniform layer of Ag nanoparticles. Subsequently the wafers were transferred to an etchant solution composed of 8% HF and 0.27 M H_2O_2. After being etched for 30 min at room temperature, the wafers were washed using 1 M diluted HNO_3 to remove the Ag catalyst and then washed with 0.1 M NaOH solution for 10 min to remove the oxide sheath. After being thoroughly washed with water, the as-prepared mpSiNWs were detached from the Si substrate by sonicating treatment, collected and re-dispersed in 5 mL water.

Preparation of RhNP@mpSiNW hybrid. 90 μL of 1 wt% $RhCl_3$ was added to the as-prepared mpSiNWs solution (adding 45, 90 and 135 μL of the $RhCl_3$ solution resulted in RhNP@mpSiNW with RhNP loading of 3.7, 7.4 and 11.1 μg/mm², respectively). Then excess amount of 0.1 wt% $NaBH_4$ solution was added to the solution slowly at 4°C during stirring in order to prepare RhNP@mpSiNW nanohybrid. The resultant solution was stirred for another 30 min to ensure full loading of the RhNPs. The

obtained RhNP@mpSiNW nanohybrid was collected, washed and re-dispersed in 1 mL water.

Preparation of RhNP@mpSiNW/GC electrode. GC electrodes were mechanically polished with 1, 0.3 and 0.05 mm alumina slurry and then washed in water, ethanol and water for 5 min sequentially. GC electrodes were then dried with nitrogen stream. The RhNP@mpSiNW solution was thoroughly mixed with Nafion solution (0.5 wt%) at 1 : 1 ratio (v/v). The RhNP@mpSiNW hybrid modified GC electrodes were obtained by drop costing 3 μL of the mixed solution onto GC electrode.

Preparation of the RhNP loaded GC electrode. Various amounts (45, 90 and 135 μL) of 1 wt% of $RhCl_3$ were added to 5 mL water. Then excess amount of 0.1 wt% $NaBH_4$ solution was added slowly at 4°C under stirring to form RhNPs. The resultant solution was stirred for another 30 min, washed and re-dispersed in 1 mL water. RhNP loading is similar to the process of RhNP@mpSiNW hybrid loading.

1. Chen, W., Cai, S., Ren, Q., Wen, W. & Zhao, Y. Recent advances in electrochemical sensing for hydrogen peroxide: a review. *Analyst* **137**, 49–58 (2012).
2. Wang, J. Electrochemical biosensors: Towards point-of-care cancer diagnostics. *Biosens. Bioelectron.* **21**, 1887–1892 (2006).
3. Wang, J. Electrochemical glucose biosensors. *Chem. Rev.* **108**, 814–825 (2008).
4. Frew, J. & Hill, H. A. Electrochemical biosensors. *Anal. Chem.* **59**, 933A–944A (1987).
5. Rodriguez, M. C. & Rivas, G. A. An enzymatic glucose biosensor based on the codeposition of rhodium, iridium, and glucose oxidase onto a glassy carbon transducer. *Anal. Lett.* **34**, 1829–1840 (2001).
6. Miscoria, S. A., Barrera, G. D. & Rivas, G. A. Glucose biosensors based on the immobilization of glucose oxidase and polytyramine on rodhinized glassy carbon and screen printed electrodes. *Sens. Actuators B.* **115**, 205–211 (2006).
7. Miscoria, S. A., Barrera, G. D. & Rivas, G. A. Analytical performance of a glucose biosensor prepared by immobilization of glucose oxidase and different metals into a carbon paste electrode. *Electroanalysis.* **14**, 981–987 (2002).
8. Chang, H. *et al*. Strongly coupled rhodium/graphene hybrids for H_2O_2 oxidation with ultra-low potential and enhanced activity. *ChemElectroChem* **1**, 1–4 (2014).
9. Wang, K., Xu, J.-J. & Chen, H.-Y. A novel glucose biosensor based on the nanoscaled cobalt phthalocyanine-glucose oxidase biocomposite. *Biosens. Bioelectron.* **20**, 1388–1396 (2005).
10. Ozoemena, K. I., Mashazi, P. N. & Nyokong, T. Tetracarboxylic acid cobalt phthalocyanine SAM on gold: potential applications as amperometric sensor for H_2O_2 and fabrication of glucose biosensor. *Electrochim. Acta.* **52**, 177–186 (2006).
11. Rodriguez, M. C. & Rivas, G. A. Highly selective first generation glucose biosensor based on carbon paste containing copper and glucose oxidase. *Electroanalysis.* **13**, 1179–1184 (2001).
12. Hua, M. Y. *et al.* The intrinsic redox reactions of polyamic acid derivatives and their application in hydrogen peroxide sensor. *Biomaterials.* **32**, 4885–4895 (2011).
13. Dong, S. J., Zhou, M. & Zhai, Y. M. Electrochemical sensing and biosensing platform based on chemically reduced graphene oxide. *Anal. Chem.* **81**, 5603–5613 (2009).
14. Shan, C. S. *et al*. Direct electrochemistry of glucose oxidase and biosensing for glucose based on graphene. *Anal. Chem.* **81**, 2378–2382 (2009).
15. Wang, J., Musameh, M. & Lin, Y. H. Solubilization of carbon nanotubes by nafion toward the preparation of amperometric biosensors. *J. Am. Chem. Soc.* **125**, 2408–2409 (2003).
16. Wang, J. & Musameh, M. Carbon nanotube/teflon composite electrochemical sensors and biosensors. *Anal. Chem.* **75**, 2075–2079 (2003).
17. Lee, K. P., Manesh, K. M., Kim, H. T., Santhosh, P. & Gopalan, A. I. A novel glucose biosensor based on immobilization of glucose oxidase into multiwall carbon nanotubes–polyelectrolyte-loaded electrospun nanofibrous membrane. *Biosens. Bioelectron.* **23**, 771–779 (2008).
18. Wang, J. & Chen, Q. Enzyme microelectrode array strips for glucose and lactate. *Anal. Chem.* **66**, 1007–1011 (1994).
19. Wang, J., Liu, J., Chen, L. & Lu, F. Highly selective membrane-free, mediator-free glucose biosensor. *Anal. Chem.* **66**, 3600–3603 (1994).
20. Hahn, Y. & Olson, C. L. Amperometric enzymatic determination of total cholesterol in human serum with tubular carbon electrodes. *Anal. Chem.* **51**, 444–449 (1979).
21. Wang, J., Chen, Q. & Pedrero, M. Highly selective biosensing of lactate at lactate oxidase containing rhodium-dispersed carbon paste electrodes. *Analytica Chimica Acta.* **304**, 41–46 (1995).
22. Janasek, D., Vastarella, W., Spohn, U., Teuscher, N. & Heilmann, A. Ruthenium/rhodium modified gold electrodes for the amperometric detection of hydrogen peroxide at low potentials. *Anal Bioanal Chem.* **374**, 1267–1273 (2002).
23. Cox, J. A. & Jaworski, R. K. Voltammetric reduction and determination of hydrogen peroxide at an electrode modified with a film containing palladium and iridium. *Anal. Chem.* **61**, 2176–2178 (1989).
24. Qu, Y., Zhou, H. & Duan, X. Porous silicon nanowires. *Nanoscale.* **3**, 4060–4068 (2011).
25. Chen, H. *et al*. Lightly doped single crystalline porous Si nanowires with improved optical and electrical properties. *J. Mater. Chem.* **21**, 801–805 (2011).
26. Hochbaum, A. I., Gargas, D., Hwang, Y. J. & Yang, P. Single crystalline mesoporous silicon nanowires. *Nano Lett.* **9**, 3550–3554 (2009).
27. Cullis, A. G. & Canham, L. T. Visible light emission due to quantum size effects in highly porous crystalline silicon. *Nature* **353**, 335–338 (1991).
28. Lin, V. S.-Y., Motesharei, K., Dancil, K.-P. S., Sailor, M. J. & Ghadiri, M. R. A porous silicon-based optical interferometric biosensor. *Science* **278**, 840–843 (1997).
29. Stewart, M. P. & Buriak, J. M. Chemical and biological applications of porous silicon technology. *AdV. Mater.* **12**, 859–869 (2000).
30. Tasciotti, E. *et al*. Mesoporous silicon particles as a multistage delivery system for imaging and therapeutic applications. *Nat. Nano-technol.* **3**, 151–157 (2008).
31. Li, Y. Y. *et al*. Polymer replicas of photonic porous silicon for sensing and drug delivery applications. *Science* **299**, 2045–2047 (2003).
32. Etienne, M. *et al*. Molecular transport into mesostructured silica thin films: electrochemical monitoring and comparison between *p6m*, $P6_3/mmc$, and *Pm3n* structures. *Chem. Mater.* **19**, 844–856 (2007).

Acknowledgments

This work was financially supported by grants from the Chinese Thousand Talents Program (YZBQF11001) and the National Natural Science Foundation of China (21371178).

Author contributions

X.F. developed the concept and coordinated the project. Z.S. and H.C. performed the research, analyzed the data and wrote the paper. C.X. and W.Z. contributed to the SEM and TEM characterizations.

Additional information

Supplementary information accompanies this paper at http://www.nature.com/scientificreports

Competing financial interests: The authors declare no competing financial interests.

How to cite this article: Song, Z., Chang, H., Zhu, W., Xu, C. & Feng, X. Rhodium Nanoparticle-mesoporous Silicon Nanowire Nanohybrids for Hydrogen Peroxide Detection with High Selectivity. *Sci. Rep.* **5**, 7792; DOI:10.1038/srep07792 (2015).